

COMPLETE MUON COOLING CHANNEL DESIGN AND SIMULATIONS*

C. Yoshikawa[#], C. Ankenbrandt, R. P. Johnson, Muons, Inc., Batavia, IL 60510, U.S.A.
 Y. Derbenev, V. Morozov, JLAB, Newport News, VA 23606, U.S.A.
 D. Neuffer, K. Yonehara, Fermilab, Batavia, IL 60510, U.S.A.

Abstract

Considerable progress has been made in developing promising subsystems for muon beam cooling channels to provide the extraordinary reduction of emittances required for an energy-frontier muon collider. However, it has not yet been demonstrated that the various proposed cooling subsystems can be consolidated into an integrated end-to-end design. Presented here are concepts to address the matching of transverse emittances between subsystems through an extension of the theoretical framework of the Helical Cooling Channel (HCC), which allows a general analytical approach to guide the transition from one set of cooling channel parameters to another.

INTRODUCTION

There has been considerable progress in developing promising subsystems for muon beam cooling channels to provide the extraordinary reduction of emittance required for an energy-frontier muon collider. A high-performance front end from the target to the cooling systems has been designed and simulated [1], and many recent advances in theory, simulation codes, and hardware development have been achieved. However, it has not yet been demonstrated that the various proposed cooling subsystems can be consolidated into an integrated end-to-end design. This paper will discuss the principles and tools to optimally match the transverse and longitudinal emittances between muon beam cooling subsystems or segments that have different characteristics. The innovation that will be exploited is the theoretical framework of the Helical Cooling Channel (HCC) [2], which allows a general analytical approach to guide the transition from one set of cooling channel parameters to another.

BASICS OF HELICAL COOLING CHANNEL THEORY

In a Helical Cooling Channel (HCC) [2,3,4], a solenoid field is augmented with a transverse helical dipole field that provides a constant dispersion along the channel as necessary for the emittance exchange that allows longitudinal cooling plus the addition of a helical quadrupole field to provide beam stability over a very large acceptance. The solenoid magnet creates an inward radial force due to the transverse momentum of the particle, while the helical dipole magnet creates an outward radial force due to the longitudinal momentum of the particle:

$$F_{h-dipole} \approx p_z \times b; b \equiv b_\phi, \quad F_{solenoid} \approx -p_\perp \times B; B \equiv B_z, \quad (1)$$

*Work supported in part by DOE STTR grant DE-SC 0007634.

[#]cary.yoshikawa@muonsinc.com

where B is the field of the solenoid, the axis of which defines the z axis and $b=b_\phi$ is the field of the transverse helical dipole. By moving to the rotating frame of the helical fields, a time- and z-independent Hamiltonian can be formed to derive the beam stability and cooling behavior [2]. The equilibrium orbit follows the equation that is the Hamiltonian solution:

$$p(a) = \frac{\sqrt{1+\kappa^2}}{k} \left[B - \frac{1+\kappa^2}{\kappa} b_\phi \right] \quad (2)$$

Conditions for transverse stability about the equilibrium orbit are:

$$0 < G \equiv \left[\left(\frac{B\sqrt{1+\kappa^2}}{pk} - 1 \right) + \left(\frac{(1+\kappa^2)^{3/2}}{pk^2} \frac{\partial b_\phi}{\partial \rho} \right) \right] \hat{D}^{-1} < R^2 \equiv \frac{1}{4} \left(1 + \frac{\left(\frac{B\sqrt{1+\kappa^2}}{pk} - 1 \right)^2}{1+\kappa^2} \right) \quad (3)$$

where the dispersion \hat{D} is:

$$\hat{D}^{-1} = \frac{a}{p} \frac{dp}{da} = \frac{\kappa^2 + (1-\kappa^2)[(B\sqrt{1+\kappa^2}/pk) - 1]}{1+\kappa^2} - \frac{(1+\kappa^2)^{3/2}}{pk^2} \frac{\partial b_\phi}{\partial \rho} \bigg|_a \quad (4)$$

in which

- p is reference momentum; a is reference radius
- $\kappa = p_{transverse}/p_z =$ helix pitch
- B is the solenoid B_z
- $k = 2\pi/\lambda$; λ is helix period, and
- $\frac{\partial b_\phi}{\partial \rho} \bigg|_a$ is the gradient of the dipole field.

The motion of particles around the equilibrium orbit is shown schematically in Figure 1.

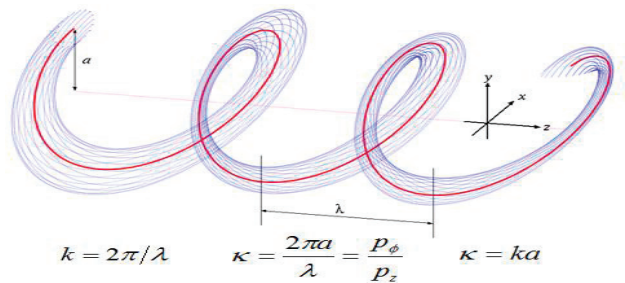


Figure 1: Schematic of beam motion in a HCC using G4beamline [5]. Reference trajectory is shown in red.

HCC MODEL FOR LONGITUDINAL EMITTANCE MATCHING TRANSITION SECTIONS

Longitudinal emittance matching in transition sections can be facilitated, subject to simultaneously satisfying

transverse stability criterion (3), by continuously varying the RF bucket area to match RF parameters from one cooling section to the next. The RF bucket area, is given by:

$$A_{bucket} \cong \frac{16}{w_{rf}} \sqrt{\frac{eV'_{max} \lambda_{RF} m_{\mu} c^2}{2\pi |\eta_H|}} \left[\frac{1 - \sin(\phi_s)}{1 + \sin(\phi_s)} \right] \quad (5)$$

where

- the term in brackets is an approximation for the moving-bucket factor
- w_{rf} is the RF frequency in radians/second
- V'_{max} is the maximum E-field voltage gradient
- λ_{rf} is the RF wavelength
- m_{μ} is the mass of the muon
- ϕ_s is the synchronous particle RF phase, and
- η_H is the translational mobility or slip factor, derived in [2] for an HCC as:

$$\eta_H = \frac{\sqrt{1 + \kappa^2}}{\gamma \beta^3} \left(\frac{\kappa^2}{1 + \kappa^2} \hat{D} - \frac{1}{\gamma^2} \right) \quad (6)$$

where a transition gamma can be identified as:

$$\frac{1}{\gamma_T^2} = \left(\frac{\kappa^2}{1 + \kappa^2} \right) \hat{D} \quad (7)$$

Thus, in matching between sections with different longitudinal dynamics, the RF bucket area can be continually manipulated by varying any of the following: the gradient of the dipole field ($\partial b_{\phi} / \partial \rho|_a$), the reference momentum (p), the accelerating phase (ϕ_s), the transition gamma γ_T , or the maximum gradient (V'_{max}).

HCC MODEL FOR TRANSVERSE EMITTANCE MATCHING TRANSITION SECTIONS

In the case of transverse matching, equation (2) would be used to compute the evolution of the solenoid B and helical dipole b_{ϕ} fields between cooling segments, where the helical dipole gradient $\partial b_{\phi} / \partial \rho|_a$ would be subject to constraint (3).

DEMONSTRATION OF ADIABATIC EVOLUTION AND BREADTH OF APPLICABILITY

Analytic guiding principles will drive simulations, which provide confidence in the designs of the transition sections. We show results of simulations that address two key factors in designing transition sections in a generalized way:

1. The ability to adiabatically transition the fields and manipulate the reference particle as desired.
2. The ability to create magnetic channels that are characteristically much different from the conventional HCC to demonstrate the generality of the theory.

Adiabatic Turn On of a Component in the Helical Channel

The goal in this demonstration is to match from a Helical Channel consisting of a single helical dipole component into one that consists of two helical dipoles, the second of which has a magnetic strength of -1/9 of the primary dipole. Figure 2 shows an adiabatic turn on that transforms an initially circular orbit into the desired elliptical trajectory.

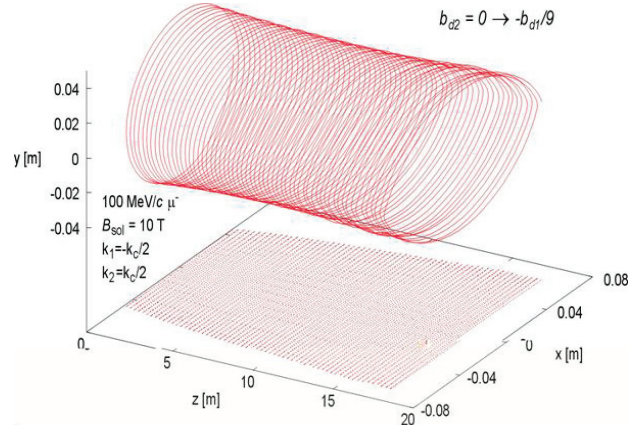


Figure 2: Adiabatic turn-on of the secondary helical dipole. The cyclotron wave number is $k_c = qB/cp_z$. The wave numbers k_1 and k_2 refer to the primary and secondary dipole fields, respectively.

General Applicability of the Helical Cooling Channel Theory

The HCC theory is not restricted to those necessarily having solenoidal fields. The Twin Helix [6,7], of which one coil configuration is shown in Figure 3, does not possess a solenoid field component. This is evident by the trajectories of muons on both charge signs in Figure 4. Hence, the HCC theory and its extensions can describe a wide variety of beam dynamics and is thus well suited to provide the platform from which matching sections can be designed.

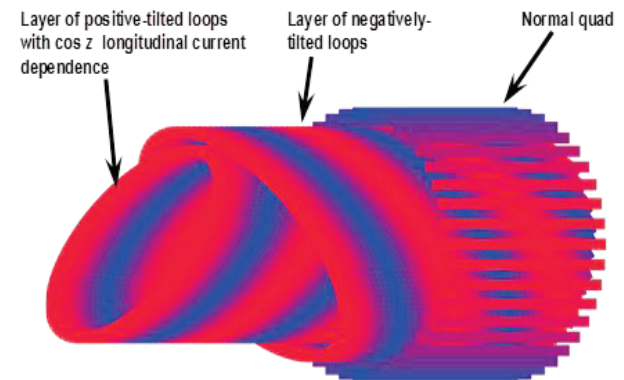


Figure 3: Possible coil configuration for Twin Helix.

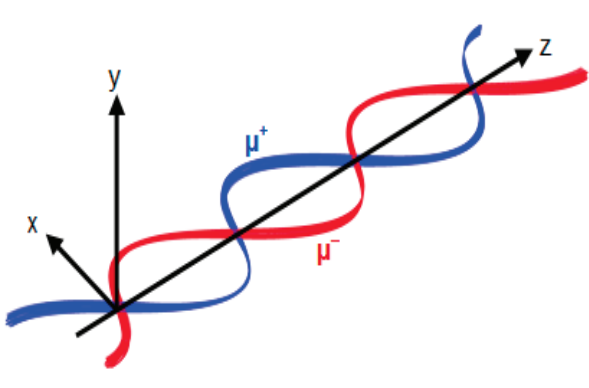


Figure 4: Planar trajectories of muons of both signs traversing Twin Helix.

Table 1: Parameters of the 8 HCC segments designed by Yonehara [8]. Simulations made with analytical EM field expressions in G4beamline [5].

	Z	b	b'	b _z	λ	v	ε _T	ε _L	ε _{6D}	ε
unit	m	T	T/m	T	m	GHz	mm rad/mm	mm	mm ³	Transmission
1	0	1.3	-0.5	-4.2	1.0	0.325	20.4	42.8	12900	
2	40	1.3	-0.5	-4.2	1.0	0.325	5.97	19.7	415.9	0.92
3	49	1.4	-0.6	-4.8	0.9	0.325	4.01	15.0	10.8	0.86
4	129	1.7	-0.8	-5.2	0.8	0.325	1.02	4.8	2.0	0.73
5	219	2.6	-2.0	-8.5	0.5	0.65	0.58	2.1	3.2	0.66
6	243	3.2	-3.1	-9.8	0.4	0.65	0.42	1.3	0.14	0.64
7	273	4.3	-5.6	-14.1	0.3	0.65	0.32	1.0	0.08	0.62
8	303	4.3	-5.6	-14.1	0.3	1.3	0.32	1.0	0.07	0.60

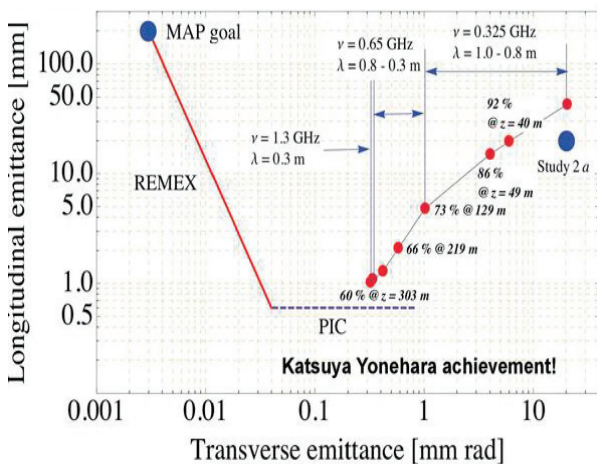


Figure 5: Fernow-Neuffer plot for emittance evolution of the 8 HCC segments in Table 1, as simulated using G4beamline [8].

THE EIGHT SEGMENT HCC CHALLENGE

A study [8] using 8 segments of the HCC achieved a 6d emittance reduction by a factor of about 190,000! The study utilized analytic expressions for the fields in

G4beamline [8] with parameters described in Table 1. The evolution of the transverse and longitudinal emittances through the HCC segments are also given in Table 1 and are also plotted as red dots in Figure 5. Forty percent of the beam is lost in the 303 m long channel. About 22% of the beam is lost due to muon decay while the rest of the loss is due to emittance mismatches. We will apply our proposed techniques to match emittances between the HCC segments to reduce the losses and demonstrate the effectiveness of the extension of the HCC theory.

SUMMARY & FUTURE

The Helical Cooling Channel theory is one that allows adiabatic changes and has applicability to channels that have a variety of characteristics, making the theory ideal to be the basis for designing transition sections in segmented cooling channels. Extensions to the HCC theory will be developed to cover the optimum matching between segments. The first demonstration of its capabilities will be applied to the 8 cooling segments conceived by Katsuya Yonehara in Table 1 and to demonstrate that the particle losses that occur due to emittance mismatches can be reduced using the newly developed techniques that extend the HCC theory.

REFERENCES

- [1] D. Neuffer, C. Ankenbrandt, R. Johnson, C. Yoshikawa, "Muon Capture, Phase Rotation, and Precooling in Pressurized RF Cavities," PAC09, WE6PFP089.
- [2] Y. Derbenev and R. Johnson, Phys. Rev. ST – Accelerators and Beams 8 (2005) 041002, <http://www.muonsinc.com/reports/PRSTAB-HCCtheory.pdf>
- [3] V. Kashikhin et al., "Magnets for the MANX Cooling Demonstration Experiment", MOPAS012, PAC07, Proc. PAC07, Albuquerque, NM, pp. 461-463(2007).
- [4] S.A. Kahn et al., "Magnet Systems for Helical Muon Cooling Channels", Proc. PAC07, Albuquerque, NM, pp. 443-445(2007).
- [5] G4beamline, T. Roberts, <http://www.muonsinc.com>
- [6] V. Morozov, "EPIC Simulations," Muon Accelerator Program Winter Meeting, JLAB, February 28, 2011 to March 4, 2011.
- [7] V.S. Morozov, Y.S. Derbenev, A. Afanasev, R.P. Johnson, "Epicyclic Twin-Helix Ionization Cooling Simulations." IPAC11, WEPZ009.
- [8] K. Yonehara, R. P. Johnson, M. Neubauer, Y. S. Derbenev, "A helical cooling channel system for muon colliders", IPAC10, MOPD076 <http://epaper.kek.jp/IPAC10/papers/mopd076.pdf>